THE JOURNAL OF BIOLOGICAL CHEMISTRY VOL. 281, NO. 4, pp. 2338–2346, January 27, 2006

Identification by Mutational Analysis of Amino Acid Residues Essential in the Chaperone Function of Calreticulin*

Received for publication, July 28, 2005, and in revised form, October 28, 2005 Published, JBC Papers in Press, November 16, 2005, DOI 10.1074/jbc.M508302200

Virginie Martin[‡1], Jody Groenendyk[‡1,2], Simone S. Steiner[‡], Lei Guo[‡], Monika Dabrowska[‡], J. M. Robert Parker[‡], Werner Müller-Esterl[§], Michal Opas[¶], and Marek Michalak[‡3]

From the [‡]Membrane Protein Research Group and the Department of Biochemistry, University of Alberta, Edmonton, Alberta T6G 2H7, Canada, [§]Institute for Biochemistry, University Hospital Frankfurt, D-60590 Frankfurt, Germany, and [¶]Department of Pathology and Laboratory Medicine, University of Toronto, Toronto, Ontario M5S 1A8, Canada

Calreticulin is a Ca^{2+}-binding chaperone that resides in the lumen of the endoplasmic reticulum and is involved in the regulation of intracellular Ca^{2+} homeostasis and in the folding of newly synthesized glycoproteins. In this study, we have used site-specific mutagenesis to map amino acid residues that are critical in calreticulin function. We have focused on two cysteine residues (Cys^{88} and Cys^{120}), which form a disulfide bridge in the N-terminal domain of calreticulin, on a tryptophan residue located in the carbohydrate binding site (Trp^{302}), and on certain residues located at the tip of the "hairpin-like" P-domain of the protein (Glu^{238}, Glu^{239}, Asp^{241}, Glu^{243}, and Trp^{244}). Calreticulin mutants were expressed in *crt*$^{-/-}$ fibroblasts, and bradykinin-dependent Ca^{2+} release was measured as a marker of calreticulin function. Bradykinin-dependent Ca^{2+} release from the endoplasmic reticulum was rescued by wild-type calreticulin and by the Glu^{238}, Glu^{239}, Asp^{241}, and Glu^{243} mutants. The Cys^{88} and Cys^{120} mutants rescued the calreticulin-deficient phenotype only partially (~40%), and the Trp^{244} and Trp^{302} mutants did not rescue it at all. We identified four amino acid residues (Glu^{239}, Asp^{241}, Glu^{243}, and Trp^{244}) at the hairpin tip of the P-domain that are critical in the formation of a complex between ERp57 and calreticulin. Although the Glu^{239}, Asp^{241}, and Glu^{243} mutants did not bind ERp57 efficiently, they fully restored bradykinin-dependent Ca^{2+} release in *crt*$^{-/-}$ cells. This indicates that binding of ERp57 to calreticulin may not be critical for the chaperone function of calreticulin with respect to the bradykinin receptor.

The endoplasmic reticulum (ER)[4] plays a critical role in the folding of secretory and membrane-associated proteins and glycoproteins (1). The ER contains several unique groups of molecular chaperones, including disulfide isomerase and its homolog ERp57, immunophilins, the Hsp70 and Hsp90 family of proteins, and the lectin-like chaperones calreticulin and calnexin (1). These chaperones and "folding sensors" play a central role in protein quality control in the ER (1, 2). ERp57 catalyzes disulfide bond exchange in substrates that are bound to calreticulin or calnexin (3). Calreticulin and calnexin are homologous proteins that both interact with monoglucosylated, trimmed intermediates of the *N*-linked core glycans on newly synthesized glycoproteins (4–6).

Biochemical and structural studies have demonstrated that calreticulin comprises three distinct structural domains: the amino-terminal N-domain, which is globular, the central P-domain, which is folded into an "extended arm," and the carboxyl-terminal C-domain (7). NMR (8), structural modeling (9, 10), and biochemical studies (11, 12) have indicated that, together, the globular N-domain and the "extended arm" P-domain of calreticulin form a functional protein-folding unit (9). The N-domain of calreticulin contains a carbohydrate binding site (13) and one disulfide bond (14). In a recent study, site-specific mutation of histidine residues in calreticulin revealed that His^{153}, which is located in the N-domain of the protein, is essential for its chaperone function (12). The "extended arm" structure of the P-domain is involved in the association of calreticulin with ERp57, a thiol-disulfide oxidoreductase that is a close homolog of protein-disulfide isomerase (15–17).

Calreticulin deficiency is embryonic lethal, and cells derived from calreticulin knockout embryos have impaired Ca^{2+} homeostasis (11). For example, in calreticulin-deficient cells, folding of the bradykinin receptor is altered, and this impairs its ability to initiate $InsP_3$-dependent Ca^{2+} release (11). The $InsP_3$-dependent Ca^{2+} release is, however, fully restored in calreticulin-deficient cells that express recombinant calreticulin (11, 12). Therefore, in this study, we used restoration of bradykinin-dependent Ca^{2+} release from the ER to compare the function of several site-specific calreticulin mutants with that of wild-type calreticulin. We focused on two cysteine residues that form a disulfide bridge in the N-domain of calreticulin, on a centrally located tryptophan residue in the carbohydrate binding site, and on several residues located at the tip of the "extended arm" of the protein's P-domain. We have identified two tryptophan residues that are critical for the chaperone function of calreticulin: Trp^{302}, which is located in the carbohydrate binding pocket and Trp^{244}, which is found at the tip of the P-domain's extended arm. In contrast, mutation of the cysteine residues disrupted the chaperone function only partially. We have also identified four amino acid residues at the tip of the "extended arm" of the P-domain that are critical in the formation of an ERp57-calreticulin complex.

EXPERIMENTAL PROCEDURES

Materials—Trypsin, malate dehydrogenase (MDH), bradykinin, and Dulbecco's modified Eagle's medium were from Sigma. Fetal bovine serum was from Invitrogen. SDS-PAGE reagents and molecular weight makers were from Bio-Rad. Effectene Transfection reagent and Ni^{2+}-nitrilotriacetic acid-agarose beads were from Qiagen. CM5 sensor chips, the amine coupling kit, and the BIA evaluation analysis program were from BIAcore Inc. All chemicals were of the highest grade available.

Plasmids and Site-directed Mutagenesis—For *Escherichia coli* expression of calreticulin, the wild type full-length rabbit calreticulin gene was amplified and cloned into pBAD/glIII to generate pBAD-CRT as previously described (12). For expression in eukaryotic cells, the rab-

* This work was supported by the Canadian Institutes of Health Research. The costs of publication of this article were defrayed in part by the payment of page charges. This article must therefore be hereby marked "*advertisement*" in accordance with 18 U.S.C. Section 1734 solely to indicate this fact.

[1] These two authors contributed equally to this work.
[2] Recipient of a Studentship from the Canadian Institutes of Health Research and the Alberta Heritage Foundation for Medical Research.
[3] A Canadian Institutes of Health Research Senior Investigator. To whom correspondence should be addressed: Dept. of Biochemistry, University of Alberta, Edmonton, Alberta, Canada T6G 2H7. Tel.: 780-492-2256; Fax: 780-492-0886; E-mail: Marek.Michalak@ualberta.ca.

[4] The abbreviations used are: ER, endoplasmic reticulum; MDH, malate dehydrogenase; CRT, calreticulin; InsP3, inositol 1,4,5-trisphosphate; HA, hemagglutinin.

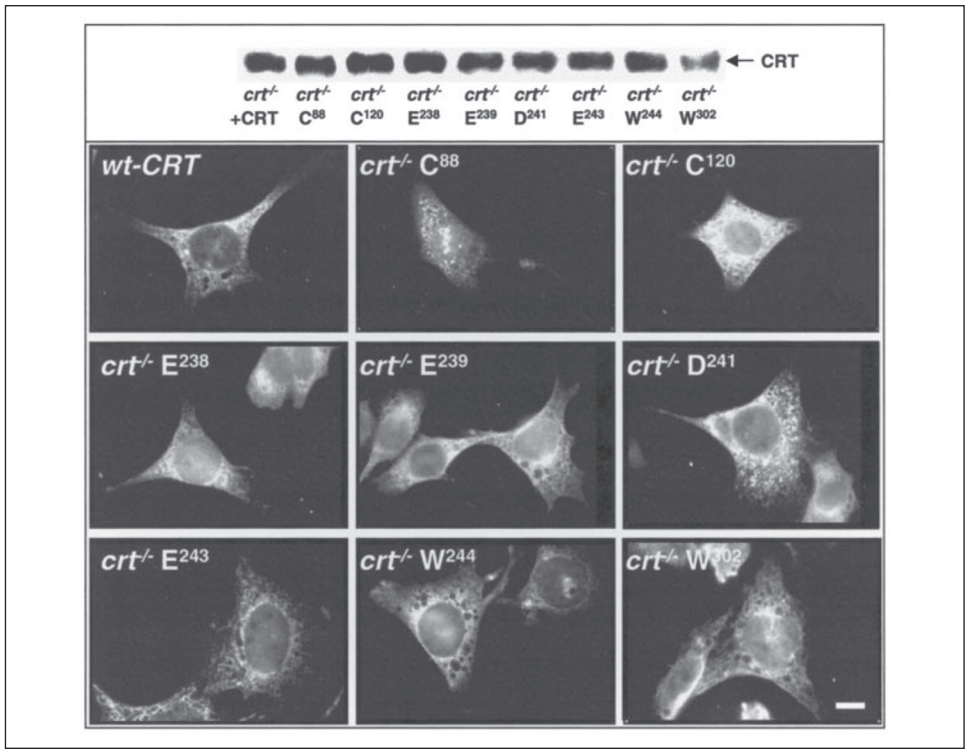

FIGURE 1. **Expression of calreticulin mutants in calreticulin-deficient mouse embryonic fibroblasts.** Western blot analysis and immunostaining of calreticulin in mouse embryonic fibroblasts was carried out as described under "Experimental Procedures" (12). *Upper panel*, proteins from calreticulin-deficient cells expressing different calreticulin mutants were lysed, separated by SDS-PAGE, transferred to nitrocellulose membrane, and probed with rabbit anti-hemagglutinin (anti-HA tag) antibody. *Lower panel*, calreticulin-deficient cells expressing different mutants were probed with anti-calreticulin antibody. *Scale bar*, 10 μm.

bit calreticulin gene was amplified and cloned into pcDNA3.1/Zeo (12). For detection of the recombinant protein, a hemagglutinin epitope (HA) tag was engineered to the C terminus of calreticulin to generate pcDNA-CRT-HA with the C-terminal ER retrieval KDEL amino acid sequence left intact (11, 12). Site-specific mutagenesis was carried out using a megaprimer polymerase chain reaction technique (18, 19) using a Gene Amp PCR system 9700 thermal cycler and *Pfx* DNA polymerase (12). The following mutants were generated: C88A, C120A, E238R, E239R, D241R, E243R, W244A, and W302A. Throughout this work, wild type calreticulin and C88A, C120A, E238R, E239R, D241R, E243R, W244A, and W302A mutants are designated as CRT-wt and CRT-C^{88}, CRT-C^{120}, CRT-E^{238}, CRT-E^{239}, CRT-D^{241}, CRT-E^{243}, CRT-W^{244}, and CRT-W^{302}, respectively.

Cell Culture, Ca^{2+} Measurements, Immunofluorescence, and Western Blot Analysis—Wild-type (K41) and calreticulin-deficient (K42) mouse embryonic fibroblasts were used in this study (11). Transfections were carried out using Effectene transfection reagent, and stable transfected cell lines were selected with Zeocin (12). The following cell lines expressing wild type calreticulin ($crt^{-/-}$-wt) or specific mutants ($crt^{-/-}$-C^{88}, $crt^{-/-}$-C^{120}, $crt^{-/-}$-E^{238}, $crt^{-/-}$-E^{239}, $crt^{-/-}$-D^{241}, $crt^{-/-}$-E^{243}, $crt^{-/-}$-W^{244}, and $crt^{-/-}$-W^{302}) were generated. Cytoplasmic Ca^{2+} concentration was measured in cells stimulated with 200 nM bradykinin (11, 12). Flow cytometry was carried out as described previously (11). For the direct addition of $InsP_3$, cells were permeabilized with digitonin (11). Ca^{2+} binding to recombinant calreticulin was measured by equilibrium dialysis (20). Immunolocalization of calreticulin and calreticulin mutants was carried out as described previously (12). For Western blot analysis, proteins were separated on SDS-PAGE (10% acrylamide), transferred to nitrocellulose membrane, and probed with rabbit anti-HA at 1:300 dilution. Anti-SERCA and anti-$InsP_3$ antibodies were used as previously described (11). Peroxidase-conjugated goat anti-rabbit IgG was used as the secondary antibody at 1:10,000 dilution.

Expression and Purification of Recombinant Proteins, Aggregation Assay, and Intrinsic Fluorescence Measurement—Proteins were expressed in Top10F′ *E. coli* cells. His-tagged proteins were purified by one-step Ni^{2+}-nitrilotriacetic acid-agarose affinity chromatography in native condition (12). Over 90% of the protein was purified to homogeneity by one-step Ni^{2+}-nitrilotriacetic acid-agarose column chromatography. Protein concentration was determined by a Beckman System 6300 amino acid analyzer or by using Bio-Rad protein assay reagent using bovine serum albumin as a standard (12). The protein aggregation assay was carried out in a mixture containing varying amounts of wild-type and mutant calreticulin at room temperature (12, 21). Samples were incubated at 42 °C in 50 mM sodium phosphate, pH 7.5, and monitored for light scattering (12, 21). The denatured MDH (0.25 μM) was suspended in a buffer containing 10 mM Tris-HCl, pH 7.0, 150 mM NaCl, 5 mM $CaCl_2$ (21), followed by the addition of wild-type or mutant calreticulin (0.25 μM). IgY was isolated from chicken egg yolk according to the protocol of the EGGstract IgY purification system and used for an aggregation assay (12). Light scattering was measured using a spectrofluorometer system C43/2000 (PTI) equipped with a temperature-controlled cell holder; the excitation and emission wavelengths were set to 320 and 360 nm, respectively (12). Intrinsic fluorescence measurements were performed at 25 °C in a spectrofluorometer system C43/2000 as described (12). The excitation wavelength was set to 286 nm, and the range of emission wavelength was set to 295–450 mm. The effect of Zn^{2+} on the intrinsic fluorescence of protein was evaluated at a wavelength of 334 nm.

Proteolytic Digestions and CD Analysis—10 μg of purified, recombinant wild-type and mutant calreticulin expressed in *E. coli* were incubated with trypsin at 1:100 (trypsin/protein; w/w), with a final trypsin concentration of 10 mg/ml (22). The proteins were separated in SDS-PAGE (10% acrylamide) and stained with Coomassie Blue (12). CD analysis was performed at 25 °C using a Jasco J720 spectropolarimeter (22).

Surface Plasmon Resonance Analysis—The sensor chip was activated, coupled, and blocked using the amine coupling kit from BIAcore. Specifically, two lanes on a CM5 chip were activated using a 1:1 mixture of *N*-hydroxysuccinimide/*N*-ethyl-*N*′-(3-dimethylaminopropyl)-carbodiimide hydrochloride for 7 min at a flow rate of 5 ml/min. Purified calreticulin or calreticulin mutants were then immobilized in 10 mM

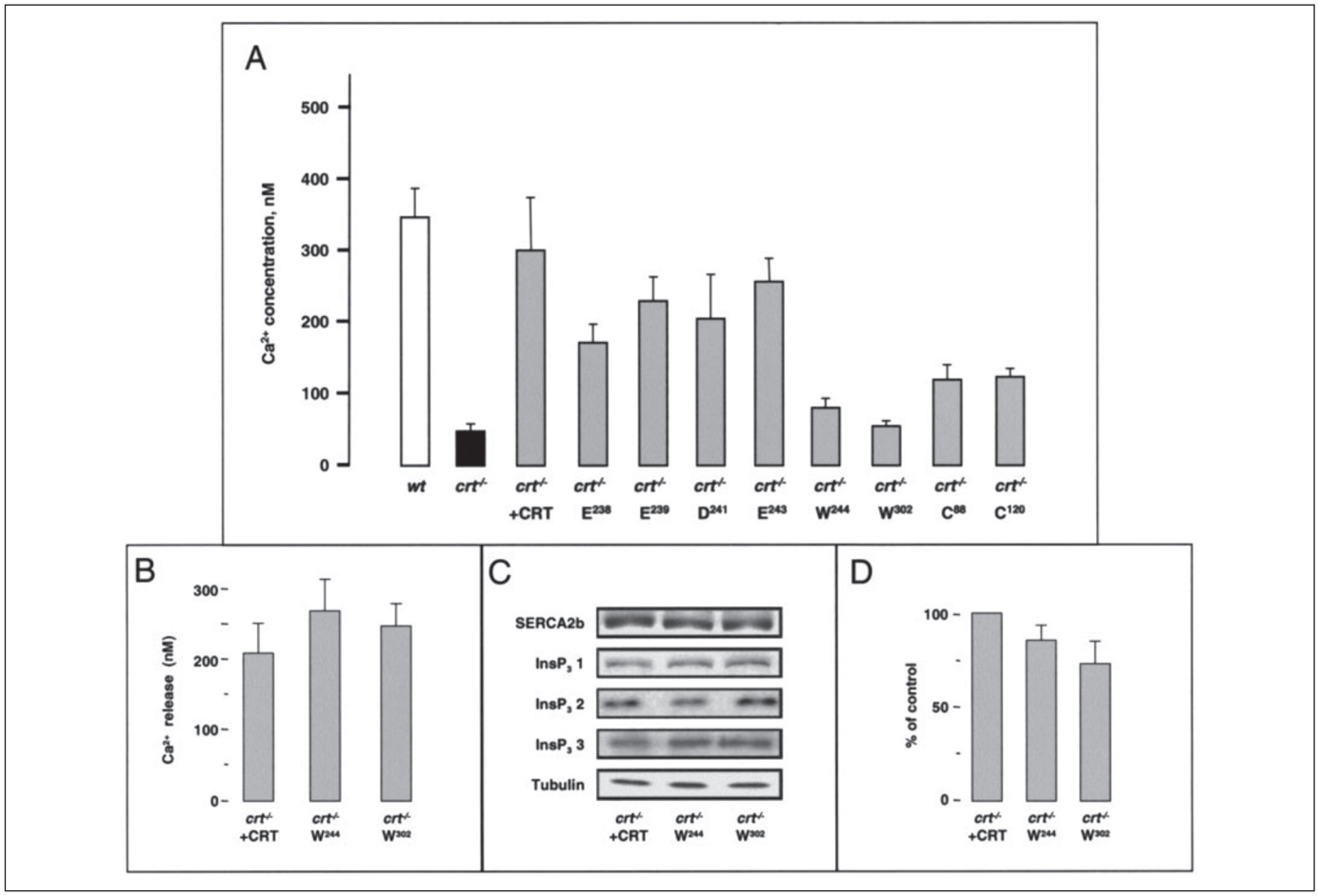

FIGURE 2. **Bradykinin-induced Ca^{2+} release in cells expressing calreticulin mutants.** *A*, cells expressing different calreticulin mutants were loaded with the fluorescent Ca^{2+} indicator fura-2 and stimulated with 200 nM bradykinin (11). *wt*, wild-type cells; $crt^{-/-}$, calreticulin-deficient cells; $crt^{-/-}$+*CRT*, calreticulin-deficient cells expressing wild type calreticulin; $crt^{-/-}$-E^{238}, cells expressing Glu^{238} mutant; $crt^{-/-}$-E^{239}, cells expressing Glu^{239} mutant; $crt^{-/-}$-D^{241}, cells expressing Asp^{241} mutant; $crt^{-/-}$-E^{243}, cells expressing Glu^{243} mutant; $crt^{-/-}$-W^{244}, cells expressing Trp^{244} mutant; $crt^{-/-}$-W^{302}, cells expressing Trp^{302} mutant; $crt^{-/-}$-C^{88}, cells expressing Cys^{88} mutant; $crt^{-/-}$-^{120}, cells expressing Cys^{120} mutant. The amount of Ca^{2+} release by bradykinin is shown. *B*, thapsigargin-releasable Ca^{2+} in calreticulin-deficient cells expressing wild type calreticulin ($crt^{-/-}$+*CRT*), in cells expressing Trp^{244} mutant ($crt^{-/-}$-W^{244}), and in cells expressing Trp^{302} mutant ($crt^{-/-}$-W^{302}). Data are mean ± S.E. ($n = 3$). *C*, SERCA2b and $InsP_3$ receptors expression in calreticulin-deficient cells. Western blot analysis was carried out as described under "Experimental Procedures." $crt^{-/-}$+*CRT*, calreticulin-deficient cells expressing wild type calreticulin; $crt^{-/-}$-W^{244}, cells expressing Trp^{244} mutant; $crt^{-/-}$-W^{302}, cells expressing Trp^{302} mutant. Anti-tubulin antibodies were used as a loading control. *D*, bradykinin receptor expression on cell surface in calreticulin-deficient cells expressing wild-type calreticulin ($crt^{-/-}$+*CRT*), in cells expressing Trp^{244} mutant ($crt^{-/-}$-W^{244}), and in cells expressing Trp^{302} mutant ($crt^{-/-}$-W^{302}). Results are presented as a percentage of control (calreticulin-deficient cells expressing wild-type calreticulin). Data are mean ± S.E. ($n = 3$).

sodium acetate buffer, pH 4, at a flow rate of 5 ml/min, and this was followed by blocking with 1 M ethanolamine, pH 8.5, for 7 min at a flow rate of 5 ml/min. A control channel on the sensor chip was activated and blocked, using amino-coupling reagent, without immobilization of protein. The protein bound to the control channel was subtracted from the protein bound to the other channels to determine specific binding. The flow buffer contained 20 mM Tris, pH 7, 135 mM KCl, 2 mM $CaCl_2$, 0.05% Tween 20, 200 μM phenylmethylsulfonyl fluoride, 100 μM benzamidine, and a mixture of protease inhibitors (23). Binding was carried out at 20 °C at a flow rate of 30 ml/min. The binding data were analyzed by nonlinear least squares curve fitting. Association and dissociation constants, k_a and k_d, were generated from the association and dissociation curves from the BIAcore experiments. ERp57 was expressed in *E. coli* and purified as previously described (24).

RESULTS

Expression of Calreticulin Mutants in Calreticulin-deficient Cells—Several domains have been identified in calreticulin by three-dimensional structural modeling (9). The N-terminal globular domain of the protein contains a carbohydrate (lectin) binding site (10), an essential histidine residue (12), and a disulfide bridge (14). The central, proline-rich P-domain of calreticulin forms an extended arm and binds ERp57 (17). To assess the functional significance of these regions in calreticulin, we carried out site-specific mutagenesis. The cysteine residues Cys^{88} and Cys^{120} (in the N-terminal domain) were mutated to alanine, to prevent formation of the disulfide bridge. A tryptophan residue located centrally in the carbohydrate binding pocket (Trp^{302}) was also mutated. Finally, a series of residues located at the tip of the "extended arm" of the P-domain (Glu^{283}, Glu^{239}, Asp^{241}, Asp^{243}, and Trp^{244}) were also mutated. Calreticulin-deficient ($crt^{-/-}$) mouse embryonic fibroblast cells (K42) were stably transfected with the expression vectors encoding these site-specific mutants, creating cell lines expressing wild-type calreticulin ($crt^{-/-}$-wt) or one of the calreticulin mutants ($crt^{-/-}$-C^{88}, $crt^{-/-}$-C^{120}, $crt^{-/-}$-E^{238}, $crt^{-/-}$-E^{239}, $crt^{-/-}$-D^{241}, $crt^{-/-}$-E^{243}, $crt^{-/-}$-W^{244}, and $crt^{-/-}$-W^{302}). The recombinant proteins were identified by an HA epitope, which was introduced at the C terminus (11, 12, 25). Western blot analysis showed that all of the transfected cells ($crt^{-/-}$-C^{88}, $crt^{-/-}$-C^{120}, $crt^{-/-}$-E^{238}, $crt^{-/-}$-E^{239}, $crt^{-/-}$-D^{241}, $crt^{-/-}$-E^{243}, $crt^{-/-}$-W^{244}, and $crt^{-/-}$-W^{302}) expressed recombinant protein (Fig. 1), and this was confirmed by immunofluorescence analysis. Using immunofluorescence, we also showed that the recombinant protein was localized in an ER-like network, by staining of the same cells with antibodies

against protein disulfide isomerase, Grp94, and calnexin (data not shown).

Bradykinin-induced Ca^{2+} Release in Cells Expressing Calreticulin Mutants—Calreticulin-deficient cells have inhibited bradykinin-dependent Ca^{2+} release, which is restored by expression of full-length recombinant calreticulin (Fig. 2*A*) (11). We took advantage of this, using the recovery of bradykinin-dependent Ca^{2+} release from the ER, in $crt^{-/-}$ cells, as a model system in which to compare the function of calreticulin and the various mutants we had generated. Fig. 2*A* shows that, as expected, bradykinin caused a rapid and transient increase in the cytoplasmic Ca^{2+} concentration in wild-type cells but not in $crt^{-/-}$ cells (11). Also, as expected, the expression of recombinant calreticulin in the $crt^{-/-}$ cells fully restored the bradykinin-dependent Ca^{2+} release (Fig. 2*A*).

Next, we measured bradykinin-dependent Ca^{2+} release in calreticulin-deficient cells ($crt^{-/-}$) expressing the various calreticulin mutants. In $crt^{-/-}$ cells expressing recombinant calreticulin with mutations at the tip of extended arm of the P-domain, bradykinin-dependent Ca^{2+} release was partially recovered (Fig. 2*A*). Specifically, expression of the mutants Glu^{238}, Glu^{239}, Asp^{241}, and Glu^{243} restored bradykinin-dependent Ca^{2+} release to 55, 75, 73, and 78% of the control, respectively (Fig. 2*A*). In contrast, expression of the Trp^{302} calreticulin mutant did not restore bradykinin-dependent Ca^{2+} release, and expression of Trp^{244} mutant restored only >10% of the activity (Fig. 2*A*). However, Trp^{244} and Trp^{302} calreticulin mutants had no effect on Ca^{2+} capacity of the ER stores (Fig. 2*B*). The expression of SERCA and $InsP_3$ receptors (Fig. 2*C*) was not altered in $crt^{-/-}$ cells expressing Trp^{244} and Trp^{302} mutants. In digitionin-permeabilized cells, $InsP_3$-induced Ca^{2+} release from ER was indistinguishable in wild-type cells and in $crt^{-/-}$ cells expressing Trp^{244} and Trp^{302} calreticulin mutants (data not shown), indicating that $InsP_3$ receptors were functional in these cells. Furthermore, flow cytometry analysis revealed that the cell surface localization of the bradykinin receptor was also not affected by in cells the expression of Trp^{244} and Trp^{302} calreticulin mutants (Fig. 2*D*). We concluded that Trp^{244} and Trp^{302} residues play an essential role in the function of calreticulin as far as folding of the bradykinin receptor is concerned.

Last, we investigated the functional consequence of mutating the cysteine residues involved in formation of the disulfide bridge in the N-domain of calreticulin (Cys^{88} and Cys^{120}). Fig. 2*A* shows that bradykinin-dependent Ca^{2+} release was increased by only 38 and 40%, compared with the control, in cells expressing the Cys^{88} and Cys^{120} mutants, respectively. These data demonstrate that the cysteine residues are also critical in determining the ability of calreticulin to function properly as a chaperone.

Effect of Calreticulin Mutants on Thermal Aggregation of MDH—In order to further examine the role of the residues Cys^{88}, Cys^{120}, Trp^{244}, and Trp^{302} in the chaperone activity of calreticulin, we exploited an *in vitro* assay used previously (12, 21). In this assay, we measured the ability of calreticulin to prevent thermal aggregation of MDH, a nonglycosylated substrate (12, 21). MDH is susceptible to heat-induced aggregation at 42 °C, as measured by light scattering, and this can be partially reversed in the presence of molecular chaperones (12, 21, 26–28). For example, full-length recombinant calreticulin effectively prevents MDH thermal-induced aggregation *in vitro* (12, 21). Using this assay, we compared the ability of mutant calreticulins to prevent thermal aggregation of MDH. To do this, we expressed the recombinant proteins in *E. coli* and purified them (Fig. 3*A*).

As previously observed, heat-induced aggregation of MDH was significantly reduced in the presence of wild-type calreticulin (21) (Fig. 3*A*). The Cys^{88}, Cys^{120}, Glu^{238}, Glu^{239}, Asp^{241}, and Glu^{243} calreticulin mutants also all prevented heat-induced aggregation of MDH and to an extent similar to that observed for the wild-type protein (data not shown). In contrast, the Trp^{302} and Trp^{244} calreticulin mutants were not effective in preventing heat-induced aggregation of MDH (Fig. 3*A*), suggesting that these residues are critical in the ability of calreticulin to prevent MDH aggregation. We also tested the effectiveness of calreticulin mutants in preventing aggregation of a glycosylated substrate, IgY (21). As expected, full-length calreticulin effectively prevented aggregation of chemically denatured IgY (Fig. 3*B*). In keeping with the results of the MDH-refolding experiments (Fig. 3*A*), Trp^{302} and Trp^{244} calreticulin mutants did not efficiently prevent aggregation of IgY (Fig. 3*B*).

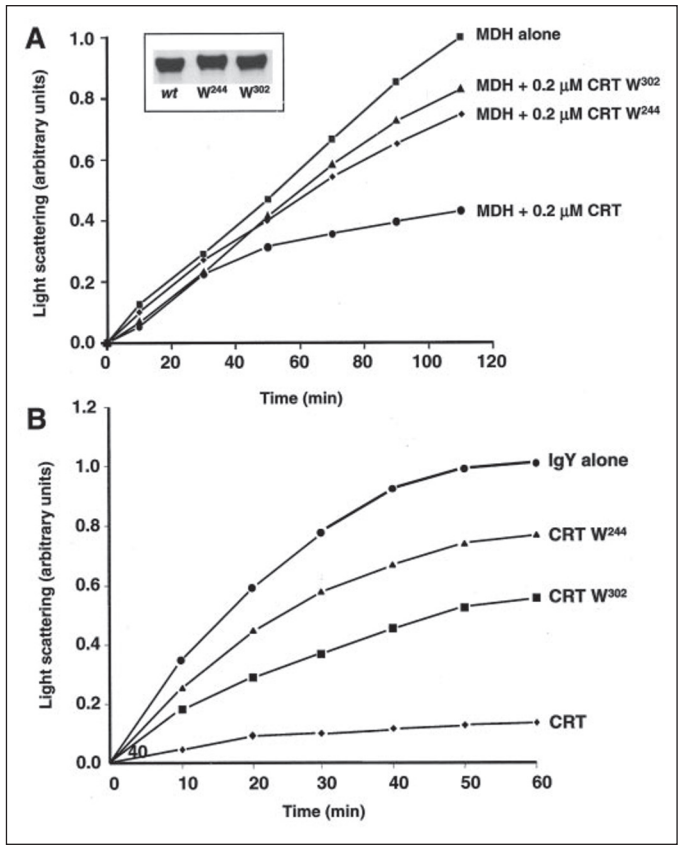

FIGURE 3. **Effects of Trp^{302} and Trp^{244} calreticulin mutants on thermal aggregation of MDH (*A*) and IgY (*B*).** MDH or IgY was incubated in the presence or absence of wild-type calreticulin or calreticulin mutants as indicated, followed by monitoring aggregation at 360 nm (21). *Box*, SDS-PAGE of recombinant wild-type (*wt*) and Trp^{244} and Trp^{302} mutants of calreticulin used for aggregation and conformational change studies is shown.

Structural Analysis of Calreticulin Mutants—Recently, we have shown that mutation of the residue His^{153} in calreticulin caused significant conformational changes in the protein (12). Since the mutations used in this study may also have affected the conformation of calreticulin, we compared the conformations of the mutants with wild-type calreticulin, using intrinsic fluorescence and limited proteolysis analysis.

The intrinsic fluorescence emission of a protein is affected by the movement of charged groups and by changes in hydrophobicity, and it provides information on changes in tertiary structure. Fluorescence emission spectra were measured for wild-type calreticulin and for calreticulin mutants at varying concentrations of Zn^{2+}. Fig. 4*A* shows that calreticulin has an emission maximum at 334 nm and that there was a progressive increase in the intensity of fluorescence in the presence of increasing concentrations of Zn^{2+} (12). This is indicative of Zn^{2+}-dependent conformational changes in the protein.

Fluorescence emission spectra for the calreticulin mutants Cys^{88}, Cys^{120}, Glu^{238}, Glu^{239}, Asp^{241}, Glu^{243}, and Trp^{302} were indistinguishable from the spectrum observed for the wild-type protein (data not shown),

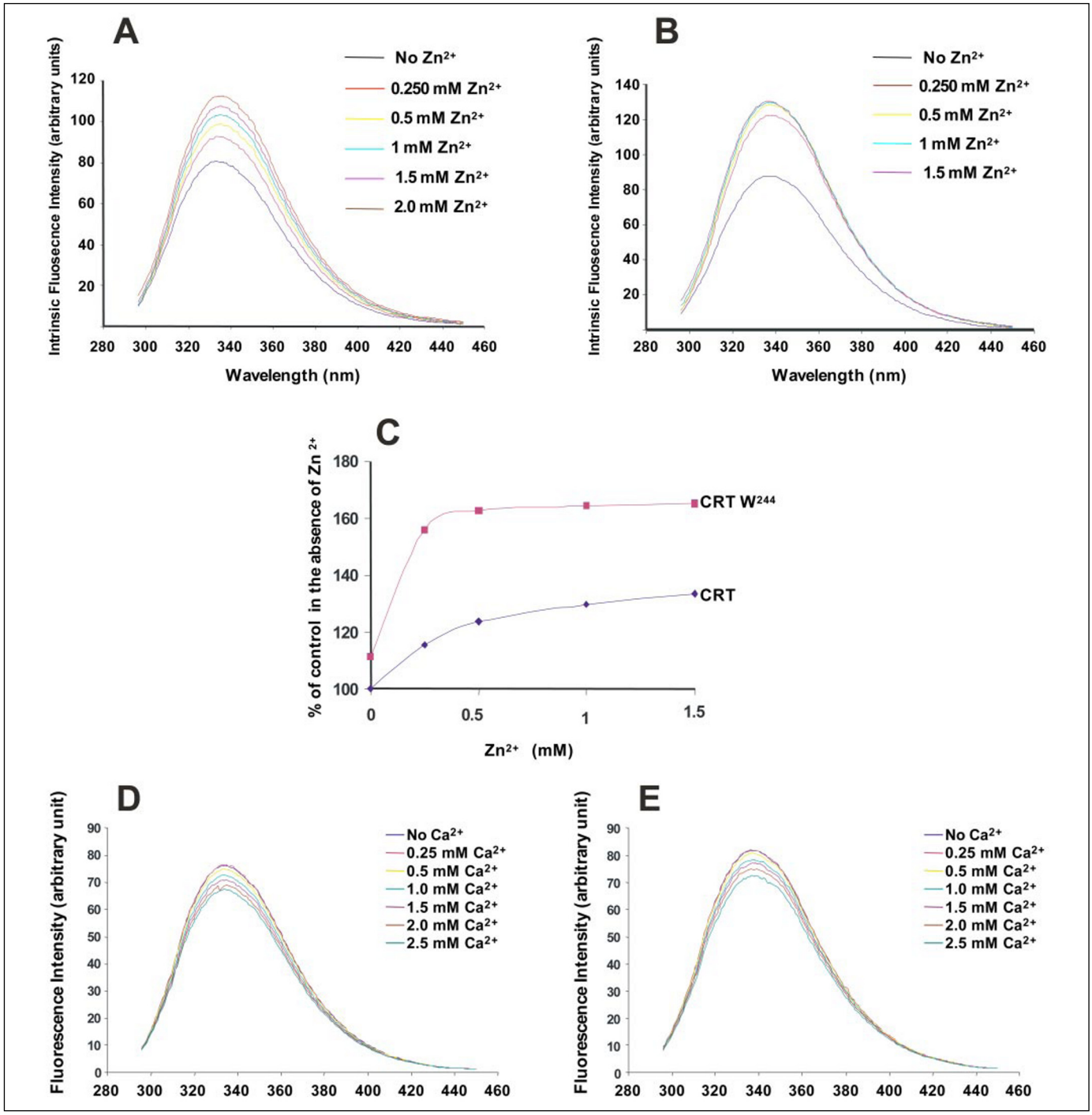

FIGURE 4. **Conformational change in Trp^{244} calreticulin mutants.** Intrinsic tryptophan fluorescence emission spectra analysis of wild-type calreticulin (*A*) and Trp^{244} mutant (*B*) was carried out as described under "Experimental Procedures," in the absence and presence of increasing concentrations of Zn^{2+}. Zn^{2+}-dependent changes in intrinsic fluorescence of wild-type and Trp^{244} mutant of calreticulin are shown in *C*. Ca^{2+}-dependent changes in intrinsic fluorescence of wild-type calreticulin (*D*) and Trp^{244} (*E*) mutant. The excitation wavelength was set at 286 nm, and the range of emission wavelength was set to 295–450 nm. *F*, CD spectra of purified wild-type calreticulin (*wtCRT*) and calreticulin mutants (Trp^{244}, Trp^{302}, Cys^{80}, and Cys^{120}). The data are plotted as molar ellipticity *versus* wavelength.

indicating that mutation of these residues in calreticulin did not significantly affect the conformation of the protein. In contrast, the mutant Trp^{244} showed larger changes in intrinsic fluorescence at lower Zn^{2+} concentrations than did wild-type calreticulin (Fig. 4*B*), the maximal change being observed by 0.25 mM Zn^{2+}. The effect of Zn^{2+} on the precise conformation of calreticulin was enhanced in the absence of the Trp^{244} residue (Fig. 4*C*). Ca^{2+}-dependent changes in intrinsic fluorescence were also measured for all mutants. There was no significant difference in the Ca^{2+}-dependent intrinsic fluorescence observed in wild-type calreticulin, in the mutant Trp^{244} (Fig. 4, *D* and *E*), and in the mutants Cys^{88}, Cys^{120}, Glu^{238}, Glu^{239}, Asp^{241}, Glu^{243}, Trp^{302} (data not shown).

To determine whether calreticulin mutations affected conformational changes in the protein, we carried out CD analysis of the purified proteins. CD spectra for Glu^{238}, Glu^{239}, Asp^{241}, and Glu^{243} were indistinguishable from the spectra obtained for wild-type calreticulin (data not shown). However, the CD spectra of wild-type calreticulin and the

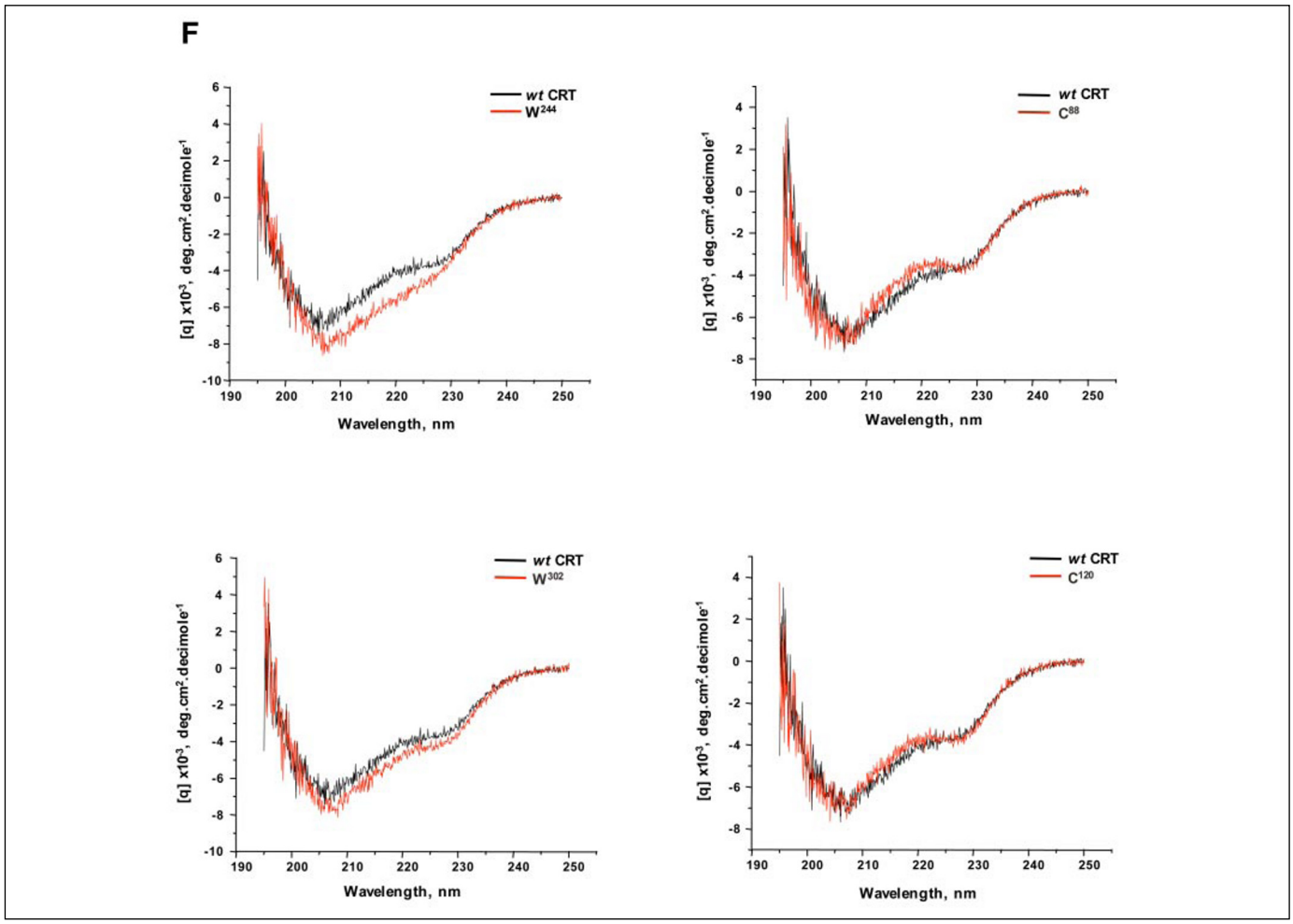

FIGURE 4—*continued*

Cys^{88}, Cys^{120}, Trp^{244}, and Trp^{302} mutants were very similar in shape but not identical (Fig. 4*F*). Trp^{244} and Trp^{302} mutants exhibited a slight increase in β-sheet-β-turn, whereas Cys^{80} and Cys^{120} showed a slight decrease in β-sheet-β-turn (Fig. 4*F*). These minor changes in conformation of Cys^{88}, Cys^{120}, Trp^{244}, and Trp^{302} mutations may have contributed, in part, to inhibition of their chaperone function.

Ca^{2+}-dependent resistance to trypsin is an excellent measure of calreticulin folding (12, 22). Therefore, we also investigated possible conformational differences between calreticulin and the calreticulin mutants using limited proteolysis. Specifically, we examined the effect of mutating the residues Cys^{88}, Cys^{120}, Glu^{238}, Glu^{239}, Asp^{241}, Glu^{243}, Trp^{244}, and Trp^{302} on calreticulin's resistance to trypsin. In agreement with our earlier observations (12, 22), in the presence of 2 mM Ca^{2+}, wild-type calreticulin is relatively resistant to trypsin digestion (trypsin/calreticulin = 1:100) (Fig. 5*A*). Mutation of Glu^{239} at the tip of the extended arm of the P-domain of calreticulin (Fig. 5*B*) and of Trp^{302} in the carbohydrate binding region (Fig. 5*C*) had no effect on the sensitivity of the protein to trypsin digestion. Both mutants were relatively resistant to digestion, similar to the wild-type protein. The mutants Cys^{88}, Cys^{120}, Glu^{238}, and Asp^{241} were also all resistant to trypsin digestion (data not shown). In contrast, the Ca^{2+}-dependent trypsin resistance of calreticulin was lost when the residues Glu^{243} and Trp^{244} were mutated (Fig. 5, *D* and *E*). Calreticulin binds Ca^{2+} at high affinity/low capacity and low affinity/high capacity sites (20), and it is possible that changes in Ca^{2+} binding to the protein could alter its sensitivity to trypsin. Therefore, we measured Ca^{2+} binding to calreticulin and the calreticulin mutants. Ca^{2+} binding to the high affinity and to the high capacity Ca^{2+} binding sites in calreticulin was not affected in any of the calreticulin mutants used in the present studies (Table 1). We conclude that the increased susceptibility to Ca^{2+}-dependent proteolysis seen in the mutants Glu^{243} and Trp^{244} indicates that mutation of these amino acid residues leads to significant alteration in calreticulin's structure.

Association of ERp57 with Calreticulin—Calreticulin associates with ERp57, a thiol-disulfide oxidoreductase and a close homolog of protein-disulfide isomerase (15, 29, 30). ERp57 binds to the tip of the hairpin-like P-domain of calreticulin (16, 17) and promotes disulfide bond formation in glycoprotein substrates (3, 31). Several of the calreticulin residues mutated in this study (Glu^{238}, Glu^{239}, Asp^{241}, Glu^{243}, and Trp^{244}) are within the region believed to contain the ERp57 binding site (16, 17, 32). We made a number of attempts to show ERp57-calreticulin interactions using GST pull-down experiments. Unfortunately, these experiments were difficult to control and reproduce because a significant amount of both calreticulin and ERp57 binds nonspecifically to the nickel affinity beads. Therefore, we used BiAcore sensor chips to test whether any of the mutated residues are involved in promoting ERp57-calreticulin association. Recombinant calreticulin and the calreticulin mutants were immobilized to a BIAcore sensor chip, and the binding of recombinant ERp57 in the flow buffer was measured. Figure 6 shows that ERp57 bound to calreticulin with high affinity. Mutation of the residue Glu^{238} in calreticulin, located at the tip of the P-domain, had no

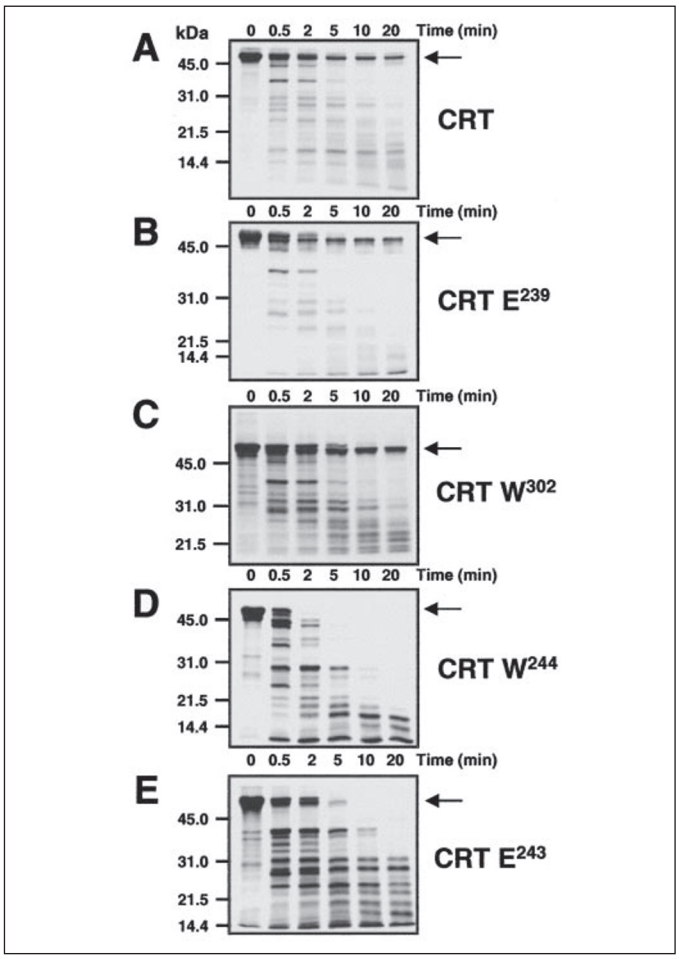

FIGURE 5. **Trypsin digestion of calreticulin and calreticulin mutants.** Calreticulin and calreticulin mutants were expressed in *E. coli*, and the purified proteins were incubated with trypsin at 1:100 (trypsin/protein; w/w) at 37 °C. Aliquots were taken at the time points indicated, and the proteins were separated by SDS-PAGE and stained with Coomassie Blue. The arrows indicate the location of calreticulin. *CRT*, calreticulin.

TABLE 1

Ca^{2+} binding to recombinant calreticulin

Ca^{2+} binding to recombinant calreticulin was measured by equilibrium dialysis (20).

Protein	mol of Ca^{2+}/ mol of protein	K_d	mol of Ca^{2+}/ mol of protein	K_d
		mM		μM
Wild-type CRT	22.0	2.0	1.0	6.0
CRT-E^{238}	20.0	1.7	0.9	6.5
CRT-E^{239}	19.0	2.1	1.1	7.0
CRT-D^{241}	20.0	1.9	1.1	7.5
CRT-E^{243}	21.5	1.8	1.0	6.5
CRT-C^{88}	19.0	1.9	1.0	6.0
CRT-C^{120}	18.5	1.9	1.0	7.0
CRT-W^{244}	22.0	2.0	1.1	7.5
CRT-W^{302}	19.0	2.2	1.0	7.0

significant effect on ERp57 binding to the immobilized protein (Fig. 6). In contrast, the mutants Glu^{239} and Glu^{243} showed significantly reduced binding of ERp57, and the mutants Asp^{241} and Trp^{244} did not bind ERp57 at all (Fig. 6). Interestingly, mutation of the Trp^{302} residue, which is localized in the N-terminal carbohydrate binding site away from the P-domain of calreticulin, significantly enhanced ERp57 binding to the protein (Fig. 6).

DISCUSSION

In this study, we used calreticulin-deficient cells to carry out a functional analysis of specific amino acid residues in calreticulin, a lectin-like chaperone in the ER. In calreticulin-deficient cells, folding of the bradykinin receptor is altered, which impairs its ability to initiate $InsP_3$-dependent Ca^{2+} release (11). This is an excellent model to investigate the function of calreticulin and to monitor the effect of specific amino acid mutations. Previously, we have used this approach to identify a histidine residue essential for the chaperone function of calreticulin (12). In the present study, we focused on amino acid residues located in the carbohydrate binding pocket of calreticulin, on the disulfide bridge in the N-domain, and on several residues at the tip of the extended arm of the P-domain. We report identification of two tryptophan residues that appear to be critical for chaperone function of calreticulin: Trp^{302} located in the carbohydrate binding pocket and Trp^{244} found at the tip of the extended arm of the P-domain. Furthermore, we identified four other amino acid residues at the tip of the extended arm of the P-domain of calreticulin that are important in the binding interaction between ERp57 and calreticulin. We also found that mutation of the cysteine residues that form the disulfide bridge also disrupted the chaperone function of calreticulin by ~60%.

Calreticulin and calnexin bind their glycoprotein substrates primarily via monoglucosylated glycans ($Glc_1Man_{7\text{-}9}GlcNAc_2$). The three-dimensional structure of the luminal domain of calnexin shows a binding site for the terminal glucose moiety of the carbohydrate within the globular N-domain of the protein (10). Molecular modeling of calreticulin, based on the structure of calnexin, indicates that these proteins may have a similar carbohydrate binding pocket (9) (Fig. 7). Structural and modeling analyses indicate that the glucose binding pocket in both proteins contains a centrally located tryptophan residue and several charged amino acid residues (9, 10). Recent *in vitro* mutational analysis of calreticulin indicates that the residues Tyr^{109}, Met^{131}, Asp^{135}, and Asp^{317}, localized in the putative carbohydrate binding site, are involved in binding of the $Glc_1Man_9GlcNAc_2$ sugar moiety (13). Asp^{135} and Tyr^{109} are probably the most important contributors toward polar interactions between the sugar and calreticulin (13). Here we show that the centrally located Trp^{302} residue in calreticulin is essential for the chaperone function of the protein *in vivo*, probably because of a critical role in carbohydrate binding. Mutation of Trp^{302} may produce important structural changes in the sugar binding site and/or in the N-terminal domain, which lead to the loss of the chaperone function of calreticulin. This is supported by our observation that the Trp^{302} mutant failed to prevent thermal aggregation of MDH. Also, the residue Trp^{302} may form a hydrogen bond with the Man_3 of the sugar moiety (13). Interestingly, although calreticulin forms functional complexes with ERp57 via its P-domain (16, 17, 32), the Trp^{302} calreticulin mutant exhibited greatly increased binding of ERp57. This indicates that a single amino acid mutation in the globular N-domain of calreticulin affects the structure and function of the distant P-domain.

The P-domain of calreticulin forms an unusual extended arm-like structure, where the C and N terminus of the domain are in close proximity (8). The structure is stabilized by three short antiparallel β-sheets. Three small hydrophobic clusters containing two tryptophan rings, including Trp^{244}, provide additional stability (8). In this study, mutation of Trp^{244} resulted in one of the most severe effects on calreticulin function. The Trp^{244} mutant of calreticulin was unable to restore bradykinin-dependent Ca^{2+} release in calreticulin-deficient cells, it did not prevent thermally induced aggregation of MDH, and it did not bind ERp57. Biophysical studies of this mutant of calreticulin suggested that conformational changes might be responsible for its loss of chaperone activity and lost ability to form a complex with ERp57. Fig. 8 shows that Trp^{244} plays a critical role in determining the structure of the tip of the extended arm in the P-domain of calreticulin (8). The indole rings of

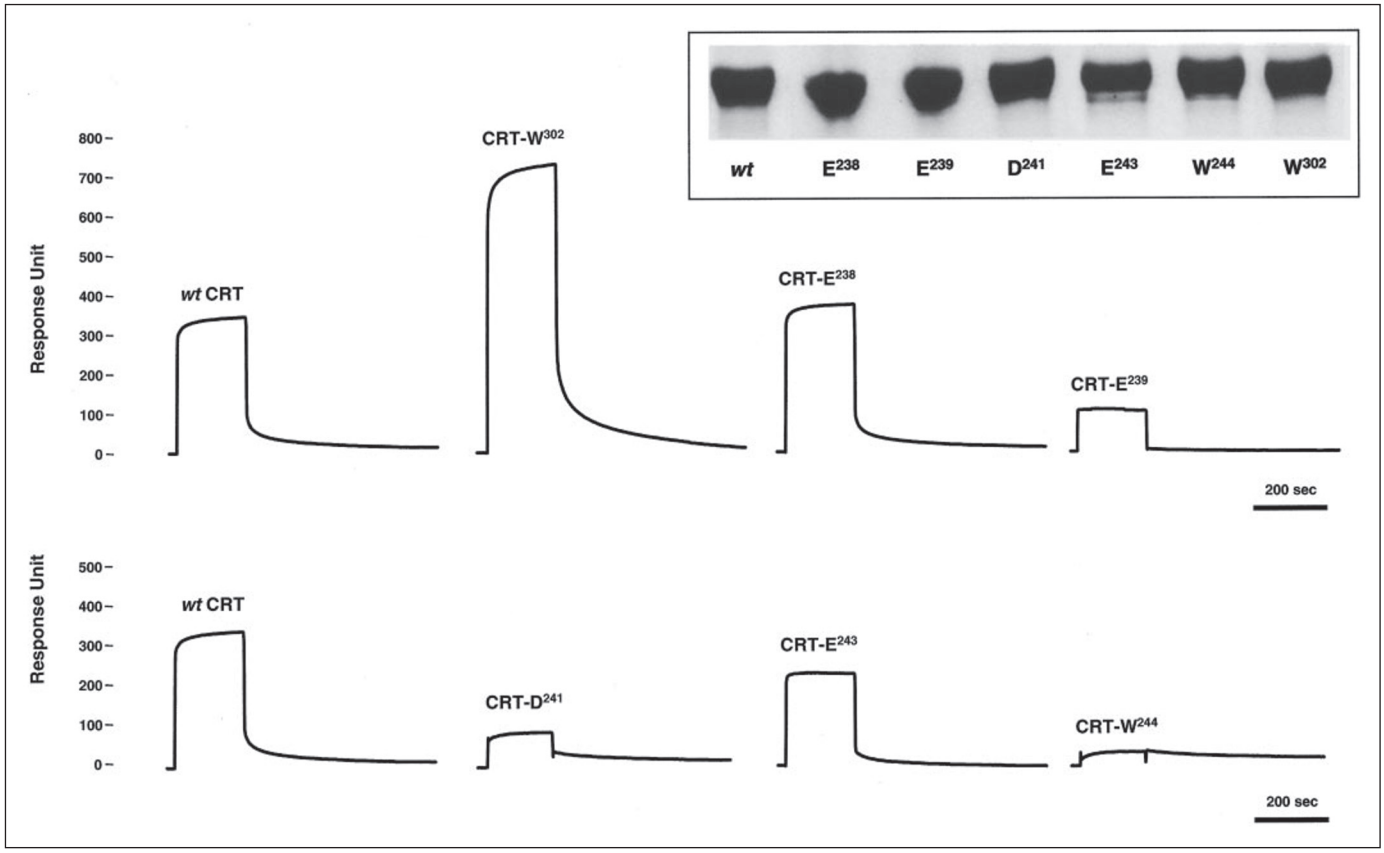

FIGURE 6. **Analysis of interactions between ERp57 and calreticulin by surface plasmon resonance.** Recombinant ERp57 was injected over immobilized calreticulin (*CRT*) or calreticulin mutants as described under "Experimental Procedures." SDS-PAGE of recombinant wild-type (*wt*) and calreticulin mutant is shown.

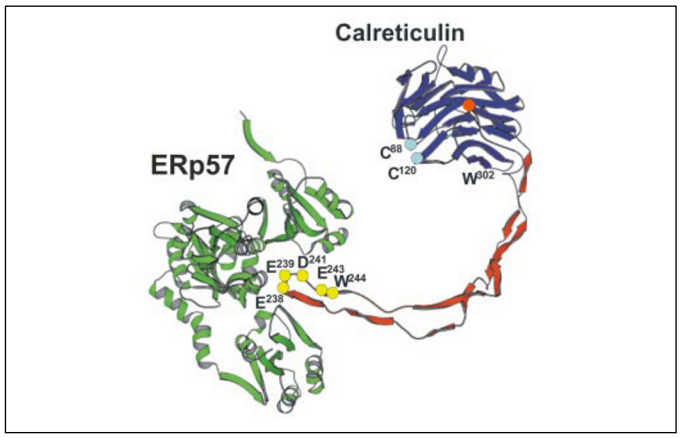

FIGURE 7. **A model of interaction of ERp57 and calreticulin and the location of the mutated amino acid residues.** ERp57 may be made of three domains connected by two loops. The loops may be bent to form a pocket surrounded by two site domains. An arginine-rich pocket of the ERp57 structure formed by three domains may slide over the tip of the P-domain (in *red*) of calreticulin to form structural and functional complexes. The location of Glu^{238}, Glu^{239}, Asp^{241}, Glu^{243}, and Trp^{244} at the tip of the P-domain, Trp^{302} in the carbohydrate putative pocket, and Cys^{88} and Cys^{120} at the surface of the N-domain to form the disulfide bond are indicated by yellow, orange, and green balls, respectively. The N- and P-domain of calreticulin are modeled based on the NMR studies of the P-domain of calreticulin (8) and crystallographic studies of calnexin (10).

residues Trp^{244} and Trp^{236} provide essential stability for the P-domain and the region involved in binding of ERp57 (Fig. 8*A*). The mutant Trp^{244} has a disturbed structure in this region, probably creating an unstable cavity (Fig. 8, *B* and *D*). This, in turn, must have a significant effect on ability of the substrate (carbohydrate) to bind to the globular N-domain of calreticulin.

NMR and biochemical analyses of the P-domain of calreticulin indicate that the tip of the extended arm binds ERp57 (16, 17, 32). NMR studies revealed that ERp57 may bind to a region of calreticulin encompassing residues 251–255 (16). We investigated several amino acid residues at the tip of the P-domain to determine their role in ERp57-calreticulin interactions (for the location of specific residues, see Fig. 7). Mutation of Glu^{238} did not effect ERp57 binding to calreticulin, whereas the mutants Asp^{241} and Trp^{244} did not bind any measurable ERp57, and the mutants Glu^{239} and Glu^{243} showed significantly reduced binding of ERp57. We conclude that the negatively charged residues Glu^{239}, Asp^{241}, and Glu^{243} and the residue Trp^{244} are essential for formation of the ERp57-calreticulin complex. The residues Glu^{239}, Asp^{241}, and Glu^{243} are located on the concave side of the tip of the P-domain, and they probably provide electrostatic forces critical in formation of the complex with ERp57. It is unlikely that Trp^{244} is directly involved in ERp57-calreticulin interactions, but rather it seems to play a in role maintaining the structural stability of the tip of the P-domain. It was surprising to find that although the mutants Glu^{239}, Asp^{241}, and Glu^{243} did not bind ERp57 efficiently, they were able to fully restore bradykinin-dependent calcium release in $crt^{-/-}$ cells, suggesting that ERp57 binding to calreticulin may not be critical for its chaperone function as far as the bradykinin receptor is concerned. Glutathione *S*-transferase pull-down analysis with the P-domain of calnexin indicates that ERp57, as well as binding to calreticulin, also binds to the P-domain of calnexin (32). Interestingly, NMR analysis showed that certain single amino acid mutations on the tip of the P-domain of calnexin had no significant effect on ERp57 binding; however, double mutants did (30). In calnexin, the residues Asp^{342}, Asp^{344}, Asp^{346}, Asp^{348}, Glu^{350}, and Glu^{352} are all involved, the residues Asp^{344} and Glu^{352} being the most important (30). This is in agreement with our data that implicate Glu^{243} (in calnexin Asp^{352}) and Glu^{239} (in calnexin Asp^{344}) as critical residues for ERp57 binding to calre-

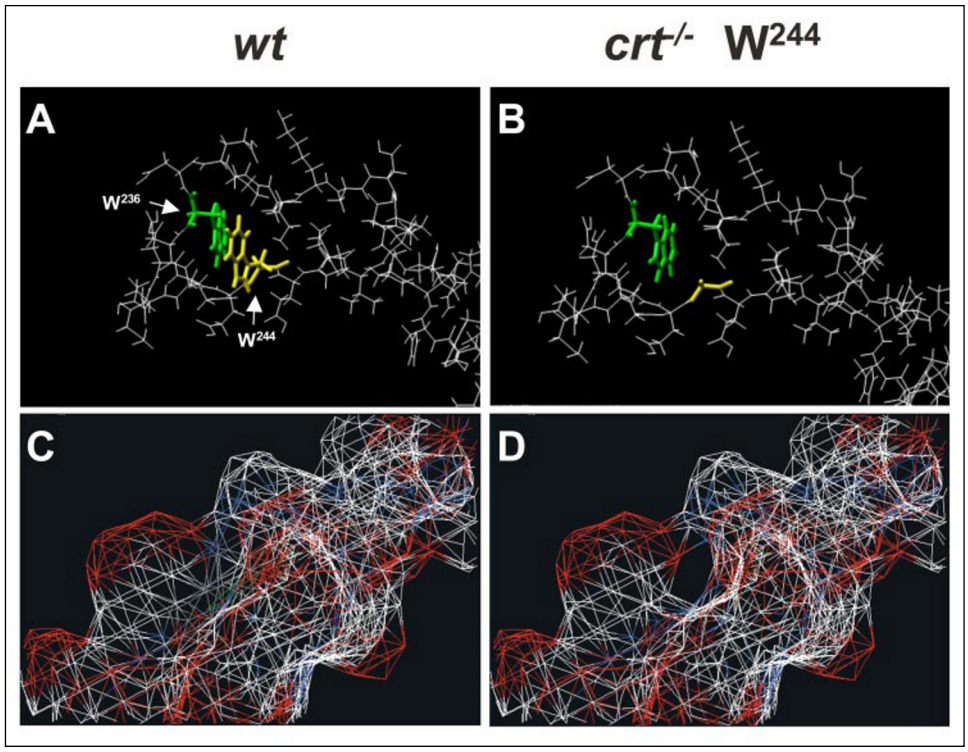

FIGURE 8. **Three-dimensional structure of the tip of the P-domain of calreticulin.** The structure of the tip of the P-domain of calreticulin is based on NMR studies (8). *A* and *C*, wild-type calreticulin; *B* and *D*, Trp^{244} calreticulin mutant. The location of the pair of interactive tryptophan residues Trp^{244} (*yellow*) and Trp^{236} (*green*) is indicated. *C* and *D*, a stereo view of the electron density around the Trp^{244}, indicating a cavity (*D*) in the P-domain with the mutated Trp^{244}.

ticulin. Thus, it appears that clusters of negatively charged residues at the tip of the P-domain, in both calreticulin and calnexin, play an important role in promoting and stabilizing association with ERp57.

In conclusion, a number of cell biological, molecular, and biophysical studies have been used to identify functionally important regions and amino acid residues in calreticulin (12) (this study). Certain amino acid residues located directly in (Trp^{302}) or near (His^{153}) (12) the carbohydrate pocket are critical for the chaperone function of the protein. Further, modification of a residue(s) in the carbohydrate binding region may have a profound effect on the structural and functional properties (mobility and stability) of the P-domain, as documented by increased ERp57 binding by the calreticulin mutant Trp^{302}. Conversely, specific amino acid residues located in the P-domain (Trp^{244}) may influence the function of the lectin-like N-domain of calreticulin. Finally, our data here indicate that the interaction between ERp57 and calreticulin, and presumably with calnexin, may not be a prerequisite for folding of all substrates.

Acknowledgments—We thank P. Scott (University of Alberta) for help with CD analysis. We thank J. Lytton (University of Calgary) for anti-SERCA antibodies and H. De Smedt and J. B. Parys for anti-$InsP_3$ receptor antibodies.

REFERENCES

1. Ellgaard, L., and Helenius, A. (2003) *Nat. Rev. Mol. Cell. Biol.* **4,** 181–191
2. Schrag, J. D., Procopio, D. O., Cygler, M., Thomas, D. Y., and Bergeron, J. J. (2003) *Trends Biochem. Sci.* **28,** 49–57
3. Zapun, A., Darby, N. J., Tessier, D. C., Michalak, M., Bergeron, J. J. M., and Thomas, D. Y. (1998) *J. Biol. Chem.* **273,** 6009–6012
4. Ou, W. J., Cameron, P. H., Thomas, D. Y., and Bergeron, J. J. M. (1993) *Nature* **364,** 771–776
5. Hammond, C., Braakman, I., and Helenius, A. (1994) *Proc. Natl. Acad. Sci. U. S. A.* **91,** 913–917
6. Ware, F. E., Vassilakos, A., Peterson, P. A., Jackson, M. R., Lehrman, M. A., and Williams, D. B. (1995) *J. Biol. Chem.* **270,** 4697–4704
7. Michalak, M., Corbett, E. F., Mesaeli, N., Nakamura, K., and Opas, M. (1999) *Biochem. J.* **344,** 281–292
8. Ellgaard, L., Riek, R., Herrmann, T., Guntert, P., Braun, D., Helenius, A., and Wuthrich, K. (2001) *Proc. Natl. Acad. Sci. U. S. A.* **98,** 3133–3138
9. Michalak, M., Robert Parker, J. M., and Opas, M. (2002) *Cell Calcium* **32,** 269–278
10. Schrag, J. D., Bergeron, J. J. M., Li, Y., Borisova, S., Hahn, M., Thomas, D. Y., and Cygler, M. (2001) *Mol. Cell* **8,** 633–644
11. Nakamura, K., Zuppini, A., Arnaudeau, S., Lynch, J., Ahsan, I., Krause, R., Papp, S., De Smedt, H., Parys, J. B., Müller-Esterl, W., Lew, D. P., Krause, K.-H., Demaurex, N., Opas, M., and Michalak, M. (2001) *J. Cell Biol.* **154,** 961–972
12. Guo, L., Groenendyk, J., Papp, S., Dabrowska, M., Knoblach, B., Kay, C., Parker, J. M. R., Opas, M., and Michalak, M. (2003) *J. Biol. Chem.* **278,** 50645–50653
13. Kapoor, M., Ellgaard, L., Gopalakrishnapai, J., Schirra, C., Gemma, E., Oscarson, S., Helenius, A., and Surolia, A. (2004) *Biochemistry* **43,** 97–106
14. Andrin, C., Corbett, E. F., Johnson, S., Dabrowska, M., Campbell, I. D., Eggleton, P., Opas, M., and Michalak, M. (2000) *Protein Expression Purif.* **20,** 207–215
15. Oliver, J. D., Roderick, H. L., Llewellyn, D. H., and High, S. (1999) *Mol. Biol. Cell* **10,** 2573–2582
16. Frickel, E. M., Riek, R., Jelesarov, I., Helenius, A., Wuthrich, K., and Ellgaard, L. (2002) *Proc. Natl. Acad. Sci. U. S. A.* **99,** 1954–1959
17. Ellgaard, L., Bettendorff, P., Braun, D., Herrmann, T., Fiorito, F., Jelesarov, I., Guntert, P., Helenius, A., and Wuthrich, K. (2002) *J. Mol. Biol.* **322,** 773–784
18. Ho, S. N., Hunt, H. D., Horton, R. M., Pullen, J. K., and Pease, L. R. (1989) *Gene* (*Amst.*) **77,** 51–59
19. Sarkar, G., and Sommer, S. S. (1990) *BioTechniques* **8,** 404–407
20. Baksh, S., and Michalak, M. (1991) *J. Biol. Chem.* **266,** 21458–21465
21. Saito, Y., Ihara, Y., Leach, M. R., Cohen-Doyle, M. F., and Williams, D. B. (1999) *EMBO J.* **18,** 6718–6729
22. Corbett, E. F., Michalak, K. M., Oikawa, K., Johnson, S., Campbell, I. D., Eggleton, P., Kay, C., and Michalak, M. (2000) *J. Biol. Chem.* **275,** 27177–27185
23. Milner, R. E., Baksh, S., Shemanko, C., Carpenter, M. R., Smillie, L., Vance, J. E., Opas, M., and Michalak, M. (1991) *J. Biol. Chem.* **266,** 7155–7165
24. Corbett, E. F., Oikawa, K., Francois, P., Tessier, D. C., Kay, C., Bergeron, J. J. M., Thomas, D. Y., Krause, K.-H., and Michalak, M. (1999) *J. Biol. Chem.* **274,** 6203–6211
25. Arnaudeau, S., Frieden, M., Nakamura, K., Castelbou, C., Michalak, M., and Demaurex, N. (2002) *J. Biol. Chem.* **277,** 46696–46705
26. Lee, G. J., Roseman, A. M., Saibil, H. R., and Vierling, E. (1997) *EMBO J.* **16,** 659–671
27. Veinger, L., Diamant, S., Buchner, J., and Goloubinoff, P. (1998) *J. Biol. Chem.* **273,** 11032–11037
28. Manna, T., Sarkar, T., Poddar, A., Roychowdhury, M., Das, K. P., and Bhattacharyya, B. (2001) *J. Biol. Chem.* **276,** 39742–39747
29. Molinari, M., and Helenius, A. (1999) *Nature* **402,** 90–93
30. Pollock, S., Kozlov, G., Pelletier, M. F., Trempe, J. F., Jansen, G., Sitnikov, D., Bergeron, J. J., Gehring, K., Ekiel, I., and Thomas, D. Y. (2004) *EMBO J.* **23,** 1020–1029
31. Oliver, J. D., van der Wal, F. J., Bulleid, N. J., and High, S. (1997) *Science* **275,** 86–88
32. Leach, M. R., Cohen-Doyle, M. F., Thomas, D. Y., and Williams, D. B. (2002) *J. Biol. Chem.* **277,** 29686–29697